

## Mechanical, Morphological, and Thermal Properties of Chemically Treated Pine Needles Reinforced Thermosetting Composites

Amar Singh Singha, Aishwarya Jyoti

Department of Chemistry, Applied Chemistry Research Laboratory, National Institute of Technology, Hamirpur 177005, Himachal Pradesh, India

Correspondence to: A. S. Singha (E-mail: assingha@gmail.com)

**ABSTRACT:** Natural fibers are widely used as reinforcement in composites. Pine needles are one of the major biowaste generated by *Pinus roxburgii* plant. This species is found abundantly in the forests of Himachal Pradesh. In this work, composites of urea–resorcinol–formaldehyde resin-reinforced with Pine needles fibers were prepared. Fibers were chemically modified to improve their compatibility with matrix. These fibers were mercerized with NaOH solution and acetylated to increase their hydrophobic character. The chemically modified fibers were characterized with Fourier transform infrared spectra,  $^{13}\text{C}$ -nuclear magnetic resonance (NMR) spectroscopy, and scanning electron microscopy. The composites were prepared with treated and untreated fibers containing 30% fibers by weight using compression molding technique. The morphology of the materials thus obtained was evaluated by scanning electron microscopy. The chemical modifications of fibers improve fiber–matrix adhesion and also have markedly effect on mechanical properties of composites. Moreover, the thermal resistance of these composites was improved on chemical modification. These results indicate that chemically modified fibers exhibit better compatibility with the polymer matrix than that of untreated fiber. © 2012 Wiley Periodicals, Inc. *J. Appl. Polym. Sci.* 000: 000–000, 2012

**KEYWORDS:** polymer composites; surface treatment; pine needles; thermosetting matrix

Received 5 April 2011; accepted 24 February 2012; published online

DOI: 10.1002/app.37636

### INTRODUCTION

Emerging community concerns and a growing environmental awareness throughout the world has forced the researchers to synthesize new green materials and processes that enhance the environmental quality of products.<sup>1–4</sup> At present, large number of industries throughout the world are initiating the design and engineering of new products with eco-friendly advantages. Sustainable development and eco-efficiency are of prime importance to the majority of international companies. In this perspective biodegradability, eco-friendliness, easy availability, and light weight, etc., have become important considerations in the fabrications of new products. At present, various workers are focusing their attention on use of lignocelluloses fibers in place of synthetic fibers in various fields especially as reinforcing fillers.<sup>5–10</sup>

Natural fiber-reinforced polymer composites have recently been preferred over composites prepared with ceramic and metal matrix because of their better properties. The use of natural fibers, derived from a number of renewable resources, as reinforcing fibers in both thermoplastic and thermoset matrix composites provides positive environmental benefits and offer numerous advantages over conventional materials including lightness, re-

sistance to corrosion, abrasion, and ease of processing, etc.<sup>11–19</sup> The commercial importance of polymers has derived intense applications in the form of composites in various fields viz. in aerospace, automotive, marine, infrastructure, military, etc. Natural fibers such as flax, hibiscus sabdariffa, pinus, jute, pine-apple leaf fiber, oil palm fiber have all been proved to be good reinforcements in thermoset and thermoplastic matrices.<sup>20–24</sup> Pine needles are abundantly found in the Himalayan region. This fiber possesses better mechanical strength<sup>16</sup> that triggered its use in composites and found applications in automotive and civil construction. Keeping in view the easy availability and many other eco-friendly advantages, we have used this fiber as reinforcing material for the preparation of Urea–resorcinol–formaldehyde (URF) resin-based composites. The composites so prepared were subjected to evaluation of their mechanical, morphological, and thermal properties.

### EXPERIMENTAL

#### Surface Modification of Pine needles

Pine needles were thoroughly washed with detergent powder and then fibers were soaked in hot distilled water for 3 h. After

**Table I.** Various Components of *Pinus roxburgii* Fiber

Sample code	Cellulose (%)	Hemicellulose (%)	Lignin (%)	Others (%)
<i>Pinus roxburgii</i>	60	20	15	5

this, fibers were dried for 48 h in air at room temperature followed by drying in a hot air oven at 105–110°C for 12 h. Dried fibers were then cut to the size of 0.5 cm. These fibers were then mercerized in 10% NaOH solution at room temperature for 3 h. After mercerization, fibers were washed with water to remove the excess soda until pH = 7 was reached and then these fibers were dried in hot air oven at 100°C for 3 h. The fibers were acetylated by immersing in pure acetic acid at room temperature for 1 h, then removed and immersed in acetic anhydride acidified with 0.1 wt % sulfuric acid for 5 min at room temperature. Finally, the samples were rinsed with water until pH = 7 was reached and dried at 100°C for 5 h. The acetylated fibers were labeled as PNaC, the mercerized ones were labeled as PNm, and unmodified fibers were labeled as PN.

**Synthesis of URF Resin.** Urea-formaldehyde resin was synthesized by the standard method developed in our Applied Chemistry research laboratory.<sup>15</sup> Urea-formaldehyde in the ratio (1.0 : 2.5) were taken by weight, in the reaction kettle and was mixed with varying ratio of resorcinol (0.5, 1.0, 1.5, 2.0, and 2.5) by weight with the help of mechanical stirrer. The reaction was carried out in an alkaline medium. Because the reaction is exothermic, proper care was taken to maintain the temperature between 50 and 60°C, for initial 2 h. Then temperature was increased to 80–85°C at pH = 5.5–6, and the mixture was heated at this temperature, till the resinification started. After the completion of resinification, the resin was cooled and ammonium chloride was added in pinch to increase the bonding between the molecules. The resin synthesized was then transferred to a specially made mould. Resin sheets of size 150 mm × 150 mm × 5.0 mm were prepared by a closed mold method as described elsewhere.<sup>4</sup> The mold was then closed and kept under pressure (4.0 MPa) until the resin was set into a hard mass. All the specimens were post cured at 120°C for 7 h.

**Preparation of Polymer Composites.** The composite samples were prepared in Compression molding machine (Santech India). The Pine needles (modified and unmodified) were mixed thoroughly with URF resin using mechanical stirrer with 30% loadings in terms of weight. The inner surfaces of molds were coated with oleic acid to avoid adhesion of the mixture to the mold and to allow easy removal of the composites. The mixture was then spread equally on the surface of the mold. Composite sheets of size 150 mm × 150 mm × 5.0 mm were prepared by compression molding technique. Composite sheets were prepared by hot pressing the mold at 130°C for 30 min. The pressure applied ranges from 3 to 4 MPa depending on the loading of reinforcing material. All the specimens were then post cured at 120°C for 12 h. The composites thus prepared were labeled using the representations as URF/PN, URF/PNm, URF/PNaC for unmodified, mercerized, and acetylated fibers respectively.

## Characterization Techniques

**Infrared Spectroscopy.** IR spectra of unmodified and modified fibers were recorded in a Fourier transform infrared spectroscopy (FTIR)-Pike Miracle ATR, Digilab Scimitar Series using Horizontal Attenuated Total Reflectance technique (FTIR-HATR) using a FTIR-BOMEM-100 Spectrometer. The FTIR-HATR technique works by passing a radiation beam through a crystal made of a high refractive index infrared-transmitting material, which is then totally internally reflected at the surface. The sample is brought in contact with the totally reflecting surface of the ATR crystal; the evanescent wave is attenuated in regions of the infrared spectrum where the sample absorbs energy. Each spectrum represents 128 co-added scans rationed against a reference spectrum obtained by recording 128 co-added scans of empty HATR cell.

**<sup>13</sup>C Magic Angle Nuclear Magnetic Resonance.** <sup>13</sup>C Magic Angle Nuclear Magnetic Resonance (<sup>13</sup>C MAS NMR) spectra of Pine fibers were recorded in a Varian Mercury Plus BB 300 MHz spectrometer operating at 75.34 MHz for <sup>13</sup>C with contact time of 1 ms and recycle time of 20 s, and 128 scans for single accumulation.

**Scanning Electron Microscopy.** The Pine fibers and its composites were observed using a scanning electron microscope (LEO VP 435). The samples were gold coated by sputtering technique and observed under different magnifications. Composite fracture surface analyses were performed after immersing the materials in liquid nitrogen for 10 min.

**Tensile Strength Test.** The tensile strength test was conducted on Computerized Universal Testing Machine (HOUNSFIELD H25KS). The specimens of dimension 100 mm × 10 mm × 5 mm were used for analysis. The tensile test was conducted in accordance with ASTM-D-3039 method. The test was conducted at the constant strain rate of 10 mm/min. Force was applied till the failure of the sample and load–elongation curve was obtained. Each sample was tested for seven times.

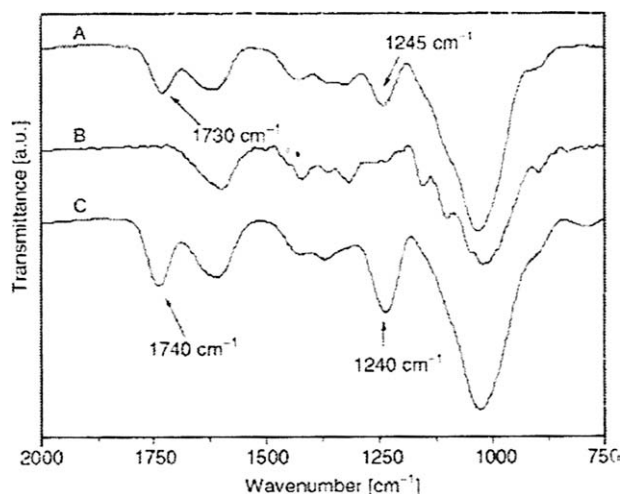


**Figure 1.** Pine needle fibers FTIR-HATR spectra: unmodified (A), mercerized (B), and acetylated (C).

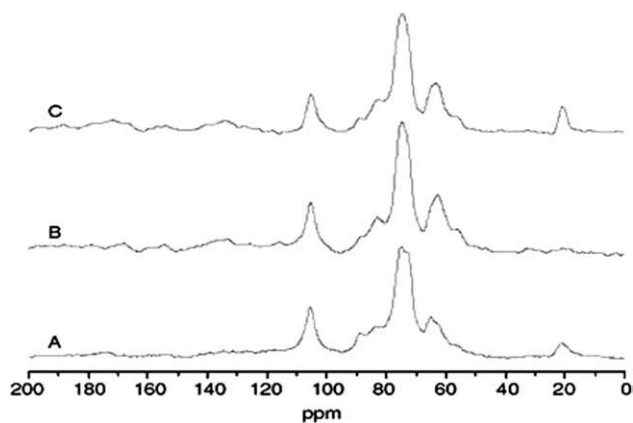
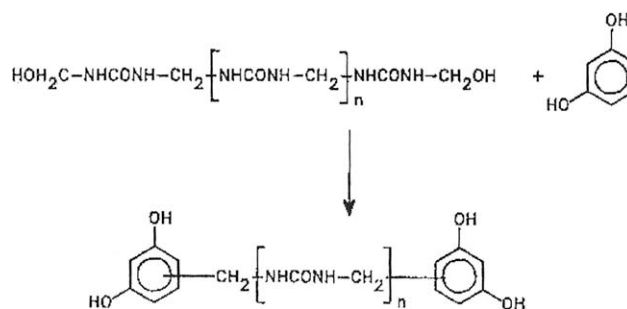


**Figure 2.** Pine needle fibers  $^{13}\text{C}$  MAS solid-state NMR spectra: unmodified (A), mercerized (B), and acetylated (C).

**Compressive Strength Test.** Compression strength of samples was tested on Computerized Universal Testing Machine. The compression test was conducted in accordance with ASTM-D-3410 method. Composite sample was held between the two platforms and the strain rate was fixed at 10 mm/min, whereas the total compression range was 7.5 mm. The compression stress was applied till the failure of sample. Total compression per unit force was noted.

**Flexural Strength Test.** Flexural strength of samples was also tested on Computerized Universal Testing Machine. The three-



**Scheme 1.** Formation of URF resin network.

point bend flexural test was conducted in accordance with ASTM-D-790 method.

**Wear Test.** The wear test of the sample was conducted on Wear & Friction Monitor (DUCOM-TR-20L). Wear resistance of composites was carried-out as per ASTM-D-3702 method. The disc was cleaned with Emery paper and it was fixed at 500 rpm. The inner diameter of steel disc was 80 mm. Initial weight of the sample was noted and the sample pin was fixed in the jaws of wear testing machine. Then machine was set to display zero wear and friction. The samples were tested with different loads varying from 1.0 to 3.0 kg. For each load, the machine was allowed to run for 15 min and the readings were recorded. After 15 min, the sample was taken out from the machine and weighed again. Then loss in weight due to abrasion was calculated and this weight loss was used as the measure of wear.

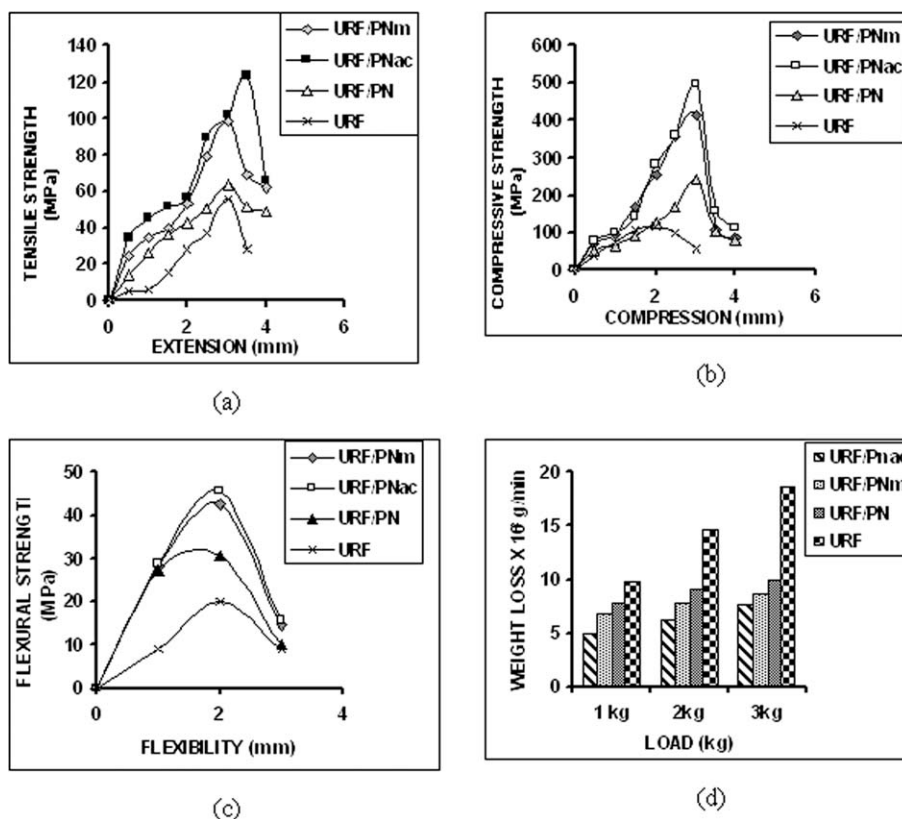


**Figure 3.** Load-extension (a), compression (b), flexibility (c), and wear resistance (d) curves of URF, URF/PN, URF/PNac, and URF/PNm composites.

**Table II.** Various Stresses Calculated from Tensile Load/Extension Curves of URF and URF-Based Composites

Sample code	Ultimate stress (MPa)	Working stress (MPa)	Yielding stress (MPa)	Fracture point (MPa)	Modulus (MPa)	SD ( $\pm$ )
URF	21.3	12.5	15.8	17.50	756.9	1.23
URF/PN	31.8	20.3	20.5	21.96	876.4	1.49
URF/PNac	44.3	21.0	27.5	28.82	1234.9	1.99
URF/PNm	38.7	19.5	22.9	24.22	1000.8	2.01

**Table III.** Various Stresses Calculated from Compressive Load/Compression Curves of URF and URF-Based Composites

Sample code	Ultimate stress (MPa)	Working stress (MPa)	Yielding stress (MPa)	Fracture point (MPa)	Modulus (MPa)	SD ( $\pm$ )
URF	46.48	29.8	34.5	38.9	1198	1.56
URF/PN	85.92	56.9	64.5	78.9	2272	1.67
URF/PNac	156	123.4	146.8	137.9	3617	1.89
URF/PNm	129	89.45	103.4	113.5	3240	2.34

**Table IV.** Various Stresses Calculated from Flexural Load/Flexibility Curves of URF and URF-Based Composites

Sample code	Ultimate stress (MPa)	Working stress (MPa)	Yielding stress (MPa)	Fracture point (MPa)	Modulus (MPa)	SD ( $\pm$ )
URF	6.06	3.20	4.90	4.10	234.6	1.93
URF/PN	9.36	6.78	7.45	8.09	335.7	2.11
URF/PNac	17.60	11.76	13.54	14.98	427.0	1.63
URF/PNm	12.04	8.98	10.23	10.99	378.9	1.5

**Stress–Strain Analysis.** Stress–strain diagram expresses a relationship between a load applied to a material and the deformation of the material, caused by the load. Stress–strain diagram was obtained from tensile, compressive, and flexural tests. Stress was calculated as usual by dividing the applied load with the initial annular cross-sectional area, whereas strain is defined as the ratio of the displacement and the initial length.

**Thermal Analysis of Samples.** Thermal analysis of natural and synthetic polymers gives us good account of thermal stability of materials. Thermogravimetric analysis and differential thermal analysis studies of samples were carried-out in nitrogen atmosphere on a thermal analyzer (Perkin-Elmer) at a heating rate of 10°C/min.

## RESULTS AND DISCUSSIONS

Chemical composition of Pine needles has been shown in Table I.<sup>16</sup>

**Table V.** Thermogravimetric Analysis of URF and URF-Based Composites

Sample code	IDT (°C)	% wt loss	FDT (°C)	% wt loss	Final residue (%)
PN	214	13.45	473	66.34	33.56
URF	239	21.48	990	85.31	14.49
URF/PN	228	27.51	781	75.63	24.67
URF/PNac	238	18.90	834	79.80	20.20
URF/PNm	231	20.82	809	81.23	17.77

### FTIR-HATR Spectra

The FTIR-HATR spectra of PN (a), PNm (b), and PNac (c) are shown in Figure 1. Compared with the curve of unmodified fiber, the spectra of mercerized and acetylated fiber have many differences. After the mercerization process, the bands at 1730 and 1245  $\text{cm}^{-1}$ , attributed to the stretching vibrations of C=O and C–O groups, respectively, disappeared. These kinds of groups are present in lignin and hemicelluloses structures. After acetylating reaction, new acetyl groups were added to the cellulose, as indicated in curve (c) with the vibrations at 1740 ( $\text{C}=\text{O}$ ) and 1240  $\text{cm}^{-1}$  (C–O). The spectrum of unmodified fiber shows an absorption peak at 1375  $\text{cm}^{-1}$  attributed to the C–H bending vibration. After esterification, the added contribution of the acetyl ( $\text{C}-\text{CH}_3$ ) stretching vibration intensifies this absorption peak.

### <sup>13</sup>C MAS NMR Spectroscopy

The mercerization and acetylation reactions of Pine cellulose were also studied by solid-state <sup>13</sup>C MAS NMR spectroscopy.

**Table VI.** DTA and DTG Analysis of URF and URF-Based Composites

Sample code	Exothermic/endothemic peaks °C ( $\mu\text{V}$ )	Exothermic peaks temperature °C (mg/min)
PN	328.0 (87); 432.0 (213)	78 (34); 209 (78); 389 (156)
URF	204 (7.8); 259 (8.2)	196 (318.7); 213 (0.25); 257 (251.1); 323 (0.137)
URF/PN	100 (2.9); 246 (34)	123 (89.6); 198 (112); 254 (114.8)
URF/PNac	289 (2.1); 478 (-12)	98 (56); 156 (178); 456 (145.3)
URF/PNm	321 (1.2); 501 (-8.9)	89 (45); 317 (221); 523 (234)

The NMR spectra of PN (a), PNm (b), and PNac (c) samples are shown in Figure 2. In spectrum (a), all noticeable signals of carbohydrate moiety carbon atoms occur between 50 and 110 ppm. The signal at 21 ppm is assigned to the  $\text{CH}_3$  carbon of the hemicellulose acetyl groups. The signals at 105 ppm (C-1), 89 ppm (C-4 of crystalline cellulose), 84 ppm (C-4 of amorphous cellulose), 75 ppm (C-5), 73 ppm (C-2 and C-3), and 64 ppm (C-6) have been observed. The intensity of C-4 signal at 89 ppm of crystalline cellulose decreased comparatively to the signal at 84 ppm, as shown by the comparison of spectrum (a) to spectra (b) and (c). The C-6 signal in (a) shifted from 64 to 62 ppm in (b) and (c). These changes may indicate that the crystalline structure of cellulose was partially disrupted by the break of  $\alpha$ -cellulose hydrogen bonds by mercerization and acetylation reactions. The degree of substitution obtained by acetylation in PNac was 0.90 (substitution of 30% in the three OH groups of each cellulose monomer). This value was obtained by area deconvolution of the peak at 21 ppm in spectrum (c) attributed to the  $-\text{CH}_3$  of the acetyl group generated by the acetylation reaction and related to the deconvoluted area of the peak at 105 ppm (C-1).

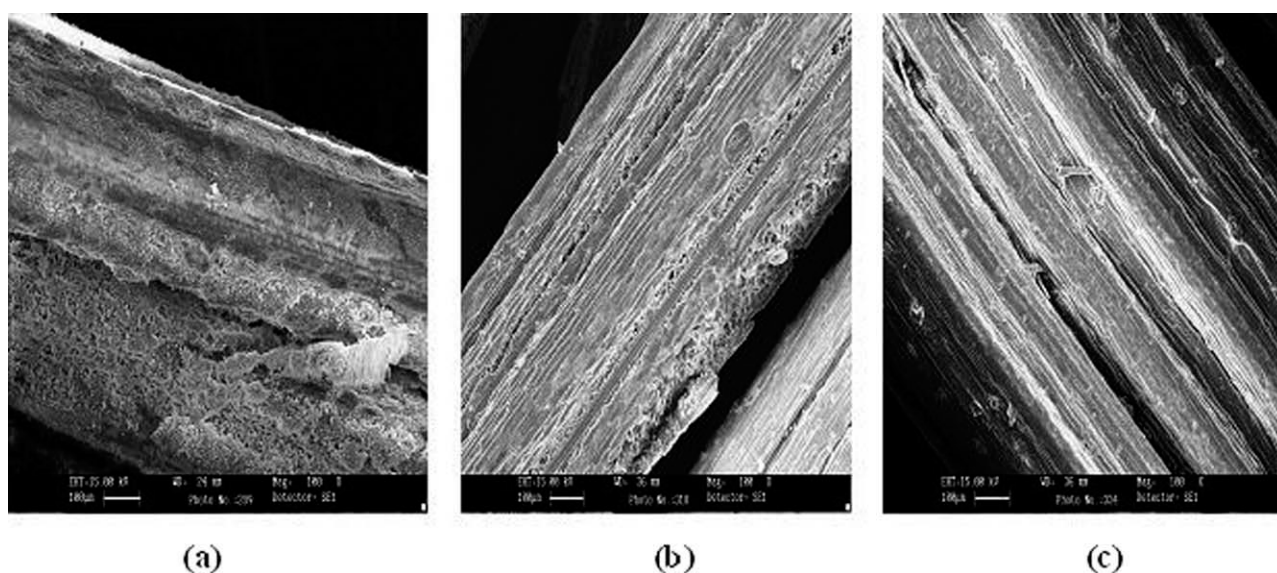
#### Mechanism of Synthesis of URF Resin

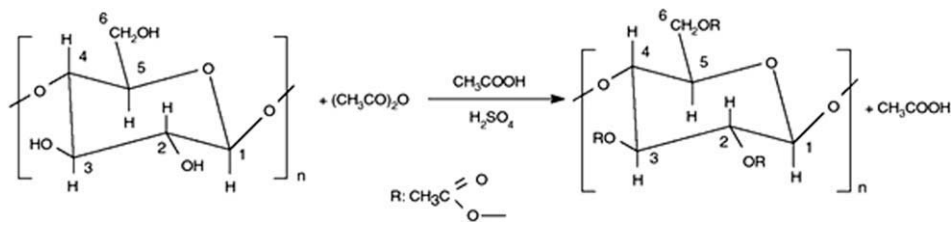
The chemical reaction is supposed to take place in two steps.<sup>16</sup> First step involves the reaction between urea and formaldehyde to form methylol urea. Because urea is tetra functional, initial reaction may leads to the formation of tetra methylol derivative

of urea which then react with resorcinol to give network of URF resin (as shown in Scheme 1).

#### Mechanical Strength

The tensile strength results of URF and its composites with unmodified and modified fibers are depicted in Figure 3(a). A gradual increase in the tensile strength was observed in URF composites reinforced with unmodified and modified fibers to that of the pure matrix. The composites with PNm presented the highest tensile strength values followed by PNac and PN. The effect of surface treatment of fiber on the tensile properties of the composite is more apparent. A good dispersion of the fibers in the polymer matrix due to change in its chemical nature produces a uniform medium for transferring the stress and as a result the tensile strength is increased. In addition, reinforcement of the interfacial phases due to chemical treatment is the main reason for the enhancement of the modulus of the system in comparison with URF and those samples with unmodified fibers. The increase in the tensile strength could be explained on the basis that after chemical treatment of fiber hemicelluloses, waxes, and other impurities are removed from the fiber and there is good fiber–matrix adhesion that leads to better tensile strength. Similar results have been obtained for compressive and flexural strengths of these composites. It has been observed that the tensile strength of URF is 55.5 MPa and URF/PN composites are 63.8 MPa, URF/PNm is 98.7 MPa, and URF/PNac is 102.3 MPa. The compressive strength has been

**Figure 4.** SEM micrographs of (a) PN, (b) PNac, and (c) PNm.



**Scheme 2.** Hydroxyl groups in the cellulose structure.

found to be 116.2 MPa for URF and 238.8, 413, and 497.6 MPa for URF/PN, URF/PNm, and URF/PNac, respectively [Figure 3(b)]. Similarly the flexural strength of these composites has the values 20.1, 30.5, 42.6, and 45.4 MPa for URF, URF/PN, URF/PNm, and URF/PNac, respectively [Figure 3(c)]. Different stresses have been calculated from tensile, compressive, and flexural curves and are presented in Tables II–IV.

Wear resistance of these composites has also been improved. It has been observed from Figure 3(d) that the wear rate of URF matrix was and URF, URF/PN, URF/PNm, and URF/PNac, respectively.

### Thermal Analysis

Thermogravimetric analysis of materials such as raw fiber, polymeric resin, and composites was studied as a function of %

weight loss vs. increase in temperature. For raw fiber, initial decomposition temperature is 214°C and final decomposition temperature is 473.0°C (Table V). In raw fiber, in the beginning various reactions such as depolymerization, dehydration, and glucosan formation took place between the temperature ranges of 26.0–200.0°C. In case of URF, it is single-stage decomposition and the initial decomposition temperature is 239.0°C and the final decomposition of the resin took place at 990.0°C (Table V). It has been observed that for raw Pine needle-reinforced composites initial decomposition temperature is 228.0°C and the final decomposition of the composite took place at 781.0°C, whereas for URF/PNac and URF/PNm, the initial decomposition started at 238 and 231°C and ended at 834 and 809°C, respectively (Table V). These values are between the degradation temperatures

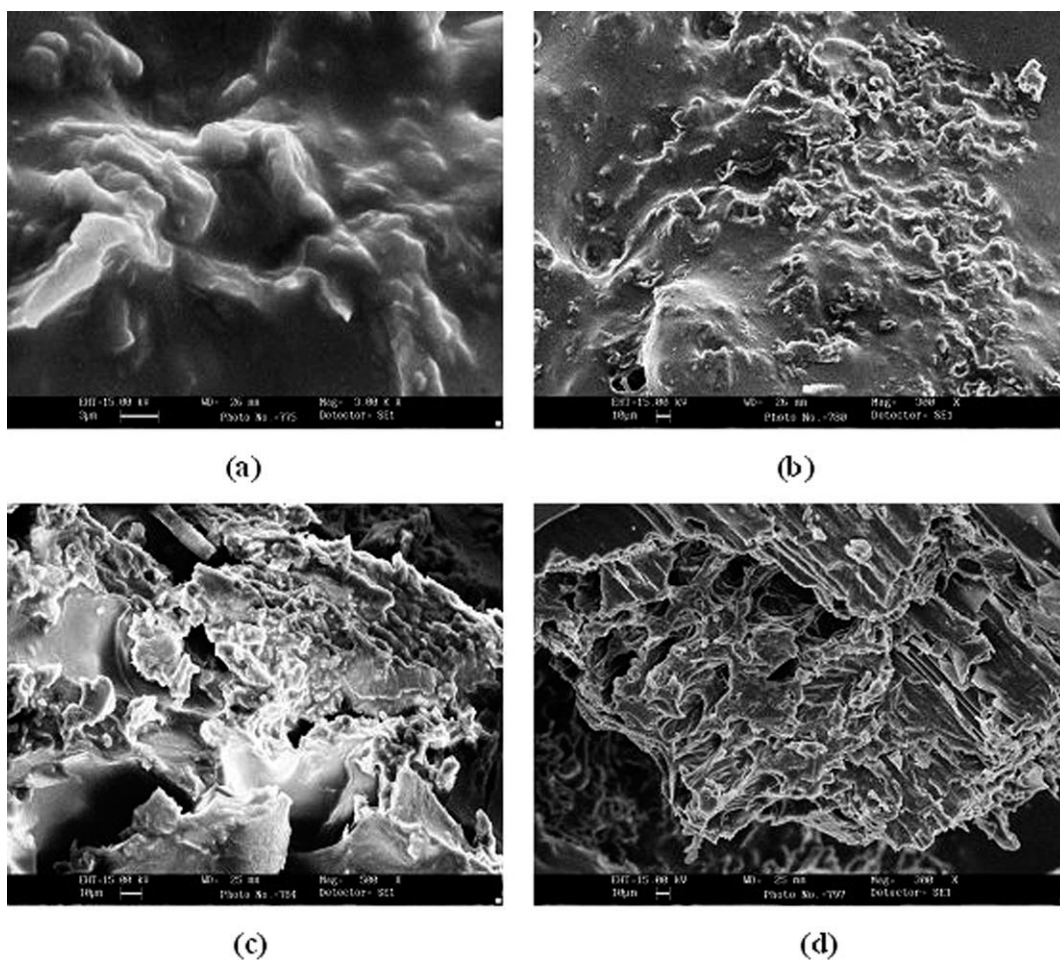


**Figure 5.** SEM micrographs of (a) URF, (b) URF/PN, (c) URF/PNac, and (d) URF/PNm.

observed for matrix and the fiber. This indicates that the presence of cellulose fibers affects the degradation process of the composites. Also, it has been found that acetylated Pine needle-reinforced composites are thermally more stable as compared with mercerized and raw fiber-reinforced composites. These studies are further supported by differential thermal analysis (Table VI). This was consistent with results reported earlier.<sup>16</sup>

### Scanning Electron Microscopy

The fiber is actually a bundle of hollow sub-fibers. The fibrillar-like structures of fibers can be observed in the fracture image scanning electron microscopy (SEM) [Figure 4(a)]. Over these structures [Figure 4(a)] was observed the presence of impurities, composed by parenchymatous cells and others constituents of the fiber such as lignin, hemicelluloses, and waxes. After alkaline treatment of Pine fibers, these surface constituents were extracted [Figure 4(b)]. Therefore, the exposition of hydroxyl groups [eq. (1)] of cellulose microfibrils occurred and this treatment should improve the acetylation process [Figure 4(c)] of all hydroxyl groups present in the cellulose structure (carbons 2, 3, and 6 in Scheme 2) in the acetylating reaction.

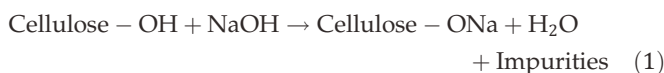


Figure 5(a–d) shows the photomicrographs of the URF-Pine needles composites. The samples were fractured in liquid nitrogen prior to observation with SEM. An increase in adhesion between the phases occurs in the composites prepared with modified fibers. The interphase adhesion allows stress transfer from matrix to the fiber and accounts for the superior mechanical strength. Adherence predominates due to increased hydrophobic character of fibers after chemical treatment. As it may be seen, the sample without chemical treatment of its fibers is pulled out easily and some holes are noticed around the fibers which imply that there are weak interactions between the filler and polymer. The breaking mode of fibers has been changed with chemical treatment and breakage of both fibers and matrix occur simultaneously.

### CONCLUSIONS

This research work presents an analysis of the interfacial behavior of lignocellulosic fiber-reinforced composites based on URF and Pine needles fibers. Two chemical modification methods (acetylation and mercerization) were applied on fibers under study. The composite samples were prepared by compression molding method with 30% fiber by weight. From the study, it has been found that chemical treatment of lignocellulosic fillers resulted in better dispersion of the filler into the polymer matrix and lead to higher impact resistance in comparison with samples containing filler with no chemical treatment. The chemical treatment of fibers improves interaction of fibers with the URF matrix, which owes to superior mechanical strength of

these composites. These composites can be future material for the production of eco-friendly materials.

### REFERENCES

1. Mukherjee, P. S.; Sukumaran, K.; Satyanarayana, K. G. *J. Mater. Sci.* **1986**, *4162*, 21.
2. Venkataswamy, M. A.; Pillai, C. K. S.; Prasad, V. S.; Satyanarayana, K. G. *J. Mater. Sci.* **1987**, *3167*, 22.
3. Bledzki, A. K.; Reihmane, S.; Gassan, J. *J. Appl. Polym. Sci.* **1996**, *1329*, 59.
4. Bledzki, A. K.; Reihmane, S.; Gassan, J. *Polym. Plastic Technol. Eng.* **1998**, *451*, 37.
5. Bledzki, A. K.; Gassan, J. *Prog. Polym. Sci.* **1999**, *221*, 24.
6. Nabi, S. D.; Jog, J. P. *Adv. Polym. Technol.* **1999**, *351*, 18.
7. Singha, A. S.; Kaith, B. S.; Sarwade, B. D. *Hungarian J. Indust. Chem.* **2002**, *289*, 30.
8. Kaith, B. S.; Singha, A. S.; Dwedi, D. K.; Kumar, D.; Kumar, S.; Dhemeniya, A. *Int. J. Plastic Technol.* **2003**, *119*, 7.
9. Kaith, B. S.; Singha, A. S.; Dwedi, D. K.; Kumar, D.; Kumar, S.; Dhemeniya, A. *Int. J. Plastic Technol.* **2004**, *299*, 8.
10. Singha, A. S.; Thakur, V. K. *Int. J. Plastic Technol.* **2007**, *835*, 11.
11. Singha, A. S.; Shama, A.; Thakur, V. K. *Int. J. Polym. Anal. Character.* **2008**, *447*, 13.
12. Singha, A. S.; Thakur, V. K. *E-J. Chem.* **2008**, *782*, 5.
13. Singha, A. S.; Thakur, V. K. *Iran. Polym. J.* **2008**, *861*, 17.
14. Singha, A. S.; Thakur, V. K. *Bull. Mater. Sci.* **2008**, *991*, 31.
15. Singha, A. S.; Thakur, V. K. *BioResources* **2008**, *1173*, 3.
16. Singha, A. S.; Thakur, V. K. *BioResources* **2009**, *292*, 4.
17. Singha, A. S.; Khanna, A. J. In *Proceeding of National Conference on Recent Advances in Innovative Materials (RAIM)*, National Institute of Technology, Hamirpur, India, **2008**; pp 208–212.
18. Sapielha, S.; Allard, P.; Zang, Y. H. *J. Appl. Polym. Sci.* **1990**, *2039*, 41.
19. Ray, D.; Sarkar, B. K.; Rana, A. K.; Bose, N. R. *Bull. Mater. Sci.* **2001**, *129*, 24.
20. Joseph, K.; Thomas, S.; Pavithran, C. *J. Reinforced Plastic Compos.* **1993**, *139*, 12.
21. Kubat, J.; Rigdahl, J.; Welander, M. *J. Appl. Polym. Sci.* **1990**, *1527*, 39.
22. Ghasemi, I.; Azizi, H.; Naeimian, N. *J. Vinyl Adhesive Technol.* **2009**, *113*, 15.
23. Tasdemir, M.; Biltekin, H.; Caneba, G. T. *J. Appl. Polym. Sci.* **2009**, *3095*, 112.
24. Joseph, K.; Mattoso, L. H. C.; Toledo, R. D.; Thomas, S.; de Carvalho, L. H.; Pothen, L.; Kala, S.; James, B. In *Natural Polymers and Agrofibrils Composites*; Frollini, E., Leao, A. L., Mattoso, L. H. C., Eds.; San Carlos, Brazil: Embrapa, USP-IQSC, UNESP, **2000**; pp 159–201.